Quadrature Chaos Shift Keying: Theory and Performance Analysis

Zbigniew Galias *Member IEEE,*
Gian Mario Maggio, *Member IEEE,*

Abstract

In this paper we propose a multilevel version of the Differential Chaos Shift Keying (DCSK) telecommunication system. The scheme, which we call Quadrature Chaos Shift Keying (QCSK), is based upon the generation of an orthogonal basis of chaotic functions. QCSK is characterized by an increased data rate with respect to DCSK, with the same bandwidth occupation, resulting in an improved spectral efficiency. The price for the performance enhancement is the increased complexity of both the transmitter and the receiver.

Keywords

QCSK (Quadrature Chaos Shift Keying), DCSK (Differential Chaos Shift Keying), Orthogonal chaotic signals, Hilbert transform.

I. Introduction

In the last few years a great research effort has been devoted towards the development of efficient chaos-based modulation techniques [1], [2], [3], [4], [5], [6], [7]. Among the several systems proposed, one of the best bit error rate (BER) performances has been achieved by the DCSK (Differential Chaos Shift Keying) scheme [4] and its variation utilizing frequency modulation, that is FM-DCSK [5]. These schemes are based upon wideband chaotic signals which under severe multipath propagation exhibit a better performance than conventional systems based on sinusoidal carriers [8]. DCSK is a transmitted-reference digital signaling scheme [9]. For each symbol period, the DCSK signal consists of a piece of chaotic waveform, followed by a non-inverted or inverted copy of itself, depending on the binary symbol ("0" or "1") to be transmitted. In [10] the first and the second part of the DCSK signal are called reference and information-bearing chip, respectively.

Recently, several different methods have been proposed in the literature to increase the data rate of DCSK [11], [12]. The simplest option consists of scaling the information and/or the reference parts of the signal. For example the information-bearing part may be multiplied by a number depending on the symbol transmitted. A more sophisticated approach uses two chaotic basis functions and divides the symbol period into four time slots in order to obtain a multilevel scheme [11]. These methods, though, achieve higher data rate by giving up some of the BER performance.

In this work we introduce a novel multilevel chaos-based communication scheme called QCSK (Quadrature Chaos Shift Keying) characterized by the same bandwidth occupation and similar BER performance as DCSK, but higher data rate.

QCSK may be considered as the chaotic counterpart of QPSK (Quadrature Phase Shift Keying) in conventional digital communications. We recall [9] that QPSK exhibits the same BER performance as BPSK (Binary Phase Shift Keying) with the same bandwidth occupation, but double data rate. This is achieved by employing a quadrature pair of sinusoidal carriers to generate an orthogonal signal basis. Since the basis components are orthogonal, they can be used to modulate information separately as for two BPSK systems sharing the same channel without (ideally) interfering with each other. Orthogonal basis functions, usually sinusoids, are used in digital communications to generate large signal constellations in order to increase the

Z. Galias is with the Institute for Nonlinear Science (INLS), UC San Diego, La Jolla, CA 92093-0402, USA, e-mail: galias@ucsd.edu. Permanent address: Dept. of Electrical Engineering, University of Mining and Metallurgy, al. Mickiewicza 30, 30–059 Kraków, Poland, e-mail: galias@zet.agh.edu.pl.

G.M. Maggio is with the Center for Wireless Communications (CWC), UC San Diego, La Jolla, CA 92093-0407, USA, e-mail: gmaggio@ucsd.edu. Corporate affiliation with STMicroelectronics, Inc., AST-La Jolla, e-mail: gian-mario.maggio@st.com.

spectral efficiency. Typical examples are M-ary PSK (Phase Shift Keying) where the phase of the transmitted signal is varied among M discrete values and QAM (Quadrature Amplitude Modulation) where both the amplitude and the phase of the reference sinusoid are varied [13].

The basic idea underlying the QCSK scheme is the generation of chaotic signals which are orthogonal in a specified time interval. This allows the creation of a basis of chaotic functions from which arbitrary constellations of chaotic signals can be constructed. For instance, in QCSK a linear combination of two chaotic basis functions is used to encode four symbols. The key point for exploiting this idea in a communication system is that one must be able to generate the chaotic basis functions starting from a single chaotic signal. The same concept holds for conventional digital communication schemes such as QPSK, where the quadrature component can be obtained from the in phase one by means of a simple phase shifter.

The paper is organized as follows. In Sec. II we recall the operation principle of DCSK comparing it to BPSK. Sec. III deals with the generation of a basis of chaotic signals. In Sec. IV we describe in details the operation of the proposed QCSK scheme. Then, in Sec. V we present the theoretical and simulation results for the performance of QCSK in the presence of noise. Finally, in Sec. VI we discuss the general case of chaos-based multilevel signaling schemes.

II. Differential Chaos Shift Keying

In DCSK two chaotic sample functions are sent for each symbol period, corresponding to one bit of information. The first function is used as a reference, while the second represents the information-bearing part of the signal. On the receiver side one observes a noisy version of the transmitted signal. The digital information is extracted by means of differentially coherent demodulation [10]. Namely, at the receiver the correlation between the two received chaotic functions is computed. The output of the correlator is then sampled according to the symbol time and a decision on the received symbol is taken.

A. DCSK versus BPSK

Differential Chaos Shift Keying is in some sense similar to the BPSK modulation scheme [9]. In BPSK one transmits a $\sin(\cdot)$ function signal or its inverted version depending on the bit of information. In principle DCSK does exactly the same except that the chaotic signal used for sending the information is different for each bit, thus one needs to send the corresponding reference signal as well in order to enable the detection at the receiver.

One of the modifications of BPSK is the QPSK scheme, which exhibits the same BER performance as BPSK, but is more efficient by having a double data rate. Basically, in QPSK a two-bit symbol is encoded as a linear combination of two orthogonal waveforms (sin and cos). In the rest of this paper we describe how this idea can be applied for increasing the data rate of DCSK.

III. Orthogonal Chaotic Signals

The first step for introducing QCSK is the generation of a (chaotic) signal orthogonal to a given chaotic reference signal in a specified time interval. Typically, two independent chaotic signals $c_1(t)$ and $c_2(t)$ (or even different segments of the same chaotic waveform) exhibit a very low cross-correlation (resp. auto-correlation) and in that sense they might be considered approximately orthogonal over a sufficiently long time interval $[0, \tau]$:

$$\int_0^\tau c_1(t)c_2(t)dt \approx 0.$$

In order to produce an orthogonal basis function useful for communication purposes we are interested in the generation of a chaotic signal y exactly orthogonal to a reference chaotic signal x, and which could be generated starting from x. This problem is the subject of the next subsection.

A. Complementary Signal

Let $x(t)$ be a chaotic reference signal defined for $t \in [0, \tau]$. Let us assume that the signal x has zero mean value[1] and that in the interval $[0, \tau]$ it admits the following Fourier expansion (with $f_0 = 0$):

$$x(t) = \sum_{k=1}^{\infty} f_k \sin(k\omega t + \varphi_k), \tag{1}$$

where $\omega = 2\pi/\tau$. Correspondingly, we denote by P_x the average power of $x(t)$ in the time interval $[0, \tau]$:

$$P_x = \frac{1}{\tau}\int_0^{\tau} x^2(t)dt = \frac{1}{2}\sum_{k=1}^{\infty} f_k^2. \tag{2}$$

We define the *complementary signal* $y(t)$, with $t \in [0, \tau]$, as the signal obtained by changing the phase of each Fourier frequency component by $\pi/2$, namely:

$$y(t) = \sum_{k=1}^{\infty} f_k \sin(k\omega t + \varphi_k - \pi/2). \tag{3}$$

The signals $x(t)$ and $y(t)$ are orthogonal in the interval $I_\tau = [0, \tau]$ and have the same power, that is:

$$x \perp y \iff \int_0^{\tau} x(t)y(t)dt = 0, \tag{4}$$

$$P_x = P_y \iff \frac{1}{\tau}\int_0^{\tau} x^2(t)dt = \frac{1}{\tau}\int_0^{\tau} y^2(t)dt. \tag{5}$$

The above properties follow from:

$$\frac{1}{\tau}\int_0^{\tau} f_k \sin(k\omega t + \varphi_k - \alpha) f_m \sin(m\omega t + \varphi_m - \beta)dt == \begin{cases} \frac{1}{2}f_k^2 \cos(\alpha + \beta) & \text{for } k = m, \\ 0 & \text{for } k \neq m. \end{cases} \tag{6}$$

An example of a chaotic signal x and the corresponding orthogonal signal y is shown in Fig. 1.

B. Relationship with Hilbert Transform

Referring to the definition (3) of the complementary signal y, we observe that by extending $x(t)$ and $y(t)$ to periodic signals with period τ, $y(t)$ represents the Hilbert transform of $x(t)$. We recall that the Hilbert transform of a real signal is obtained by introducing a $\pi/2$ phase shift in every frequency component. This property is well known and exploited for example in the context of amplitude modulation (AM) for obtaining a single (suppressed-carrier) sideband (SSB) signal [9]. Note also that the Hilbert transform preserves the spectral properties of the signal; hence we can conclude that the signals x and y have the same bandwidth occupation.

C. Practical Algorithms

So far, several methods have been developed to design finite impulse response (FIR) and infinite impulse response (IIR) digital Hilbert transformers such as the Remez exchange algorithm [14], eigenfilter method [15], and weighted least squares method [16]. Moreover, there are several methods for implementing the Hilbert transformer, including switched-capacitor implementation [17], neural network [18], and multiplierless triangular array realization [19]. Typically, these methods provide only an approximation of the Hilbert transform, as the ideal Hilbert filter impulse response extends infinitely in both directions. However, in this work rather than producing the ideal Hilbert transform, we are interested in generating the complementary signal y (given x) such that the orthogonality condition (4) is exactly satisfied over a given time interval.

We present here three methods, two of which are suitable for discrete-time signals (C.1 and C.2) and one for continuous-time signals (C.3).

[1]This assumption simply implies that the DC value of the reference signal $x(t)$ is filtered out.

C.1 Frequency Domain Approach

Given a length-K chaotic sequence $x = \{x_j\}_{j=1}^{K}$ we can generate the complementary signal $y = \{y_j\}_{j=1}^{K}$ according to the following procedure, in analogy with the AM-SSB modulation [20].

1. Subtract the mean value from the input sequence (and if necessary zero pad such that $K = 2^n$):

$$x_0 = x - \overline{x}.$$

2. Calculate the fast Fourier transform (FFT):

$$x_f = \mathcal{F}[x_0].$$

3. Create a vector h whose elements $h(j)$ have the values
- 1 for $j = 1, (K/2) + 1$,
- 2 for $j = 2, 3, \ldots, (K/2)$,
- 0 for $j = (K/2) + 2, \ldots, K$,

and calculate x_h as the element-wise product of h and x_f (this operation corresponds to eliminate the FFT coefficients associated with negative frequencies, preserving the signal energy);

4. Take the inverse FFT:

$$y = \mathcal{F}^{-1}[x_h].$$

In practice, the algorithm described can be implemented by means of a DSP (digital signal processor) unit.

C.2 Time Domain Approach

Another viable method to compute the Hilbert transform of a given discrete-time signal x is to design a FIR (Finite Impulse Response) filter approximation to the Hilbert transform operator. An FIR filter can be designed by appropriately windowing the ideal impulse response [21]:

$$h(k) = \begin{cases} \frac{2}{\pi}\frac{\sin^2(\pi k/2)}{k} & \text{for} \quad k \neq 0, \\ 0 & \text{for} \quad k = 0. \end{cases} \tag{7}$$

Note that Eq. (7) describes a noncausal filter, which means that in practice a delay m is in the filter response. Namely, the orthogonal vector y can be generated by convolution of x with h:

$$y(k) = \sum_{j=-m}^{m} x(k+j)h(j).$$

Of course, due to the finite number of taps, the FIR implementation provides an approximation of the Hilbert transform. For a discussion of the filter length selection refer to [21].

C.3 Allpass Filters

In the continuous-time domain the Hilbert transform operation may be realized by an allpass filter with unity gain and phase response equal to $\pi/2$ over a certain frequency range [22]. Typically the ideal response is approximated by means of elliptical filters. However, in practice it is hard to obtain the desired response over a sufficiently wide bandwidth. In addition, as noted above the ideal Hilbert transform filter is noncausal. In the continuous-time implementation, though, adding a delay to make the filter causal also adds a constant phase delay. This results in a linear phase component which is an undesirable effect.

D. Chaotic Signal Constellations

The main advantage of producing an orthogonal basis of chaotic functions $[x(t), y(t)]$ is that large signal sets can be generated, resulting in high spectral efficiency. Referring to (2), an orthonormal basis of chaotic sample functions over the interval $I_\tau = [0, \tau]$ can be defined as follows:

$$\mathcal{C} \equiv [c_x(t), c_y(t)] = \left[\frac{1}{\sqrt{E_\tau}}x(t), \frac{1}{\sqrt{E_\tau}}y(t)\right].$$

Chaotic signal constellations			
	s	$m_s = a_s + ib_s$	$m_s(t)$
DCSK1	s=0	1	$+c_x(t)$
	s=1	-1	$-c_x(t)$
DCSK2	s=0	i	$+c_y(t)$
	s=1	$-i$	$-c_y(t)$
QCSK1	s=0	1	$+c_x(t)$
	s=1	i	$+c_y(t)$
	s=2	$-i$	$-c_y(t)$
	s=3	-1	$-c_x(t)$
QCSK2	s=0	$(+1+i)/\sqrt{2}$	$(+c_x(t)+c_y(t))/\sqrt{2}$
	s=1	$(-1+i)/\sqrt{2}$	$(-c_x(t)+c_y(t))/\sqrt{2}$
	s=2	$(+1-i)/\sqrt{2}$	$(+c_x(t)-c_y(t))/\sqrt{2}$
	s=3	$(-1-i)/\sqrt{2}$	$(-c_x(t)-c_y(t))/\sqrt{2}$

TABLE I

CHAOTIC SIGNAL CONSTELLATIONS AND CORRESPONDING SIGNALS FOR THE CASES (A), (B), (C), (D) OF FIG. 3.

where: $E_\tau = P_x\tau$, is the energy associated with x (and y) over I_τ, such that:

$$\int_0^\tau c_x^2(t)dt = \int_0^\tau c_y^2(t)dt = 1, \tag{8}$$

(and of course: $\int_0^\tau c_x(t)c_y(t)dt = 0$). The orthonormality condition (8) implies that the energy associated with the signals $c_x(t)$ and $c_y(t)$ is constant for every interval I_τ and in particular equals unity.

A constellation of chaotic signals can then be generated as linear combinations of the basis signal c_x and c_y, that is:

$$m_s(t) = a_s c_x(t) + b_s c_y(t),$$

where the index s identifies the symbol in the signal space. Equivalently, the symbol s can be represented as a complex number[2]:

$$m_s = a_s + ib_s.$$

In this work we consider the four signal constellations shown in Fig. 3, whose analytical representations are reported in Table I. Constellations (a) and (b) are two-level signaling, the first one being the ordinary binary DCSK. The case (b) may have the advantage—with respect to conventional DCSK—that the signal transmitted is never repeated, thus resulting possibly in a low probability of interception (LPI). On the other hand, Fig. 3(c,d) show the signal constellations corresponding to two versions of a four-level QCSK chaotic signaling scheme. Finally, one can easily verify that for all cases considered:

$$\int_0^\tau m_s^2(t)dt = 1. \tag{9}$$

i.e. the information signal m_s is also characterized by constant energy, in particular equal to unity.

[2]In the rest of the paper it should be clear from the context whether we are referring to the function of time $m_s(t)$ or to the corresponding complex number m_s.

IV. Quadrature Chaos Shift Keying

The aim of this section is to illustrate the QCSK modulation scheme, whose simplified block diagram is shown in Fig. 2. For the sake of simplicity we consider here a baseband system. It is clear, though, that if the scheme is to be employed for instance for wireless communications a modulator to generate the corresponding RF passband signal is needed. Furthermore, we assume that the description of the QCSK scheme in the continuous-time domain admits an equivalent discrete-time representation. According to the sampling theorem [9] it suffices that the sampling rate $f_s \geq 2B$, where B is the max bandwidth occupation of the corresponding continuous-time signals. With these notations, a time interval Δt maps in the discrete-time domain to $\Delta k = \Delta t/t_s$, where $t_s = 1/f_s$ is the sampling time interval.

A. QCSK Modulation

In QCSK, similarly to DCSK, to send the symbol s we transmit for half symbol period the chaotic reference chip $r(t) = \sqrt{E_b}c_x(t)$ and in the second half the information-bearing chip $i(t) = \sqrt{E_b}m_s(t)$, where s denotes the symbol to be transmitted and E_b is the energy per bit. From the orthonormality condition (8) and from (9) it follows $E_b = \text{const.}$, that is the energy per bit is constant for every transmitted bit. In practice, the same result may be achieved by using the chaotic signals x and y to drive a frequency modulator, as it is done in FM-DCSK [5].

In formulae, by denoting with $T = 2\tau$ the symbol period, the QCSK transmitted signal can be expressed as:

$$S_{\text{QCSK}}(t) = \begin{cases} \sqrt{E_b}c_x(t) & \text{for} \quad 0 \leq t < T/2, \\ \sqrt{E_b}\left(a_s c_x(t - T/2) + b_s c_y(t - T/2)\right) & \text{for} \quad T/2 \leq t < T, \end{cases}$$

where for QCSK: $s = 0, 1, 2, 3$.

Referring to the block diagram in Fig. 2, the QCSK modulator consists of a chaotic generator producing the signal c_x, for each time interval $[0, T/2]$. The corresponding orthogonal signal c_y is generated by the Hilbert filter, that for simplicity we assume to introduce no extra-delay.[3] The encoder produces a linear combination of the signals c_x and c_y, depending on the symbol s to be transmitted. The latter information is provided by the Bit/Symbol converter, mapping each input bit pair to the corresponding symbol. As a result two bits of information are transmitted for each symbol period T. Then, a two-channel analog multiplexer, with switching time equal to $T/2$, is used to form the QCSK signal. Note that, although not explicitly represented in Fig. 2, the QCSK scheme must include a lowpass bandlimiting filter limiting the bandwidth of the signal to be transmitted over the channel. It is indeed clear that every physical channel possesses finite bandwidth.

B. QCSK Demodulation

The QCSK signal can be demodulated by using differentially coherent detection [10]. In this work we will assume symbol time synchronization, that is the receiver "knows" the beginning of each symbol frame (of duration T) for starting the correlation process. This is a standard assumption when analyzing a communication system [23].

Theoretically, by correlating the information-bearing part of the signal $i(t) = \sqrt{E_b}m_s(t)$ with the chaotic basis signals $c_x(t)$ and $c_y(t)$, over $[T/2, T]$, one can retrieve the complex number $m_s = a_s + ib_s$. In fact, from (4,5) it follows that:

$$a_s = \frac{1}{\sqrt{E_b}} \int_{T/2}^{T} m_s(t) c_x(t - T/2) dt,$$

$$b_s = \frac{1}{\sqrt{E_b}} \int_{T/2}^{T} m_s(t) c_y(t - T/2) dt.$$

In practice, at the receiver one observes a noisy and filtered version of the reference signal, $\tilde{r}(t)$, and of the information-bearing signal $\tilde{i}(t)$. In our analysis we assume that the only distortion affecting the received

[3] In practice this translates into the fact that if the real Hilbert transformer introduces a delay of m samples, the reference signal needs to be delayed by the same amount.

signal is additive white Gaussian noise (AWGN). Note that different sample functions of filtered noise $n(t)$ corrupt the reference and information-bearing part of the signal. Namely, the inputs of the correlator A in Fig. 2 are:

$$\tilde{r}(t-T/2) = \sqrt{E_b}\tilde{c}_x(t-T/2) = \sqrt{E_b}[c_x(t-T/2) + n(t-T/2)], \qquad t \in [T/2, T], \tag{10}$$

and:

$$\tilde{i}(t) = \sqrt{E_b}\tilde{m}_s(t) = \sqrt{E_b}[a_s c_x(t-T/2) + b_s c_y(t-T/2) + n(t)], \qquad t \in [T/2, T], \tag{11}$$

By using the corrupted chaotic reference $\tilde{c}_x(t)$ we produce an estimate of the orthogonal signal $\tilde{c}_y(t)$. In particular, by indicating with $\mathcal{H}$ the Hilbert transform operator, it follows that:

$$\begin{aligned} \tilde{c}_y(t-T/2) &= \mathcal{H}\left[\tilde{c}_x(t-T/2)\right] \\ &= \mathcal{H}\left[c_x(t-T/2) + n(t-T/2)\right] \\ &= c_y(t-T/2) + n'(t-T/2), \end{aligned}$$

where we denoted: $n'(t) = \mathcal{H}\left[n(t)\right]$. In the case of ideal Hilbert transform the statistics of the noise term n' coincide with n, that is with AWGN. We assume this to hold true also when considering an approximation by the Hilbert filter. This hypothesis is confirmed by our simulation results (see Sec. V-A).

The received information-bearing signal $\tilde{m}_s(t)$ is correlated with the noisy versions of the chaotic basis functions $\tilde{c}_x(t)$ and $\tilde{c}_y(t)$, as illustrated schematically in Fig. 2. The outputs of the correlators provide the observation signals z_a and z_b, based on which a decision about the received symbol $\tilde{s}$ is taken, once every T seconds. The decision boundaries for each signal constellation are shown in Fig. 3. Finally, the Symbol/Bit converter reconstructs the sequence of received bits.

C. Observation Signals

The noise performance of a digital communication scheme is determined by the probability distribution of the observation variables. For QCSK, if the time-varying channel varies slowly compared to the symbol rate, from (10) and (11) it follows:

$$z_a = \int_{T/2}^{T} \left[\sqrt{E_b}c_x(t-T/2) + n(t-T/2)\right] \left[\sqrt{E_b}a_s c_x(t-T/2) + \sqrt{E_b}b_s c_y(t-T/2) + n(t)\right] dt,$$

which keeping into account that c_x and c_y are orthonormal over $[T/2, T]$, reduces to:

$$\begin{aligned} z_a &= a_s E_b + \sqrt{E_b}a_s \int_{T/2}^{T} c_x(t-T/2)n(t-T/2)dt \\ &+ \sqrt{E_b}b_s \int_{T/2}^{T} c_y(t-T/2)n(t-T/2) + \sqrt{E_b}\int_{T/2}^{T} c_x(t-T/2)n(t)dt \\ &+ \int_{T/2}^{T} n(t)n(t-T/2)dt. \end{aligned} \tag{12}$$

Note that by setting $\boxed{a_s = \pm 1}$ and $\boxed{b_s = 0}$ the structure of expression (12) for the observation variable z_a coincides with the DCSK one, as reported for example in [24].

Similarly:

$$z_b = \int_{T/2}^{T} \left[\sqrt{E_b}c_y(t-T/2) + n'(t-T/2)\right] \left[\sqrt{E_b}a_s c_x(t-T/2) + \sqrt{E_b}b_s c_y(t-T/2) + n(t)\right] dt,$$

from which:

$$\begin{aligned} z_b &= b_s E_b + \sqrt{E_b} a_s \int_{T/2}^{T} c_x(t-T/2) n'(t-T/2) dt \\ &+ \sqrt{E_b} b_s \int_{T/2}^{T} c_y(t-T/2) n'(t-T/2) dt + \sqrt{E_b} \int_{T/2}^{T} c_y(t-T/2) n(t) dt \\ &+ \int_{T/2}^{T} n(t) n'(t-T/2) dt. \end{aligned} \tag{13}$$

In (12) and (13) the first term provides the desired coefficients a_s and b_s, respectively, and it is proportional to the energy per bit E_b. All the remaining terms are due to the noise on the channel. In particular, the second, third and fourth terms depend on products of the channel noise and the chaotic basis functions. According to [24] we refer to these terms as cross-products. Finally, the last term in (12) and (13) depends solely on the channel noise. In particular, this term has zero mean value but it has a non-Gaussian distribution, and it can be shown that its variance increases with the bit duration T [10]. For a detailed discussion and interpretation of the above terms we refer the reader to [24].

We anticipate that, as a refinement of the preliminary results in [7], because of the different structure of the observation variables the performance of QCSK in the presence of noise is in general slightly different from DCSK. This is discussed in details in the next section.

V. QCSK Noise Performance

In this section we report about the performance of the proposed QCSK communication scheme in the presence of additive white Gaussian noise. We consider here the discrete-time version of the QCSK scheme shown in Fig. 2. For this analysis we selected the 3-adic Rényi map:

$$f(x) = (3x+1) \mod 2 - 1,$$

as an instance of chaotic system. For each symbol period T a length-K vector x of chaotic iterates is generated. Its mean value is then subtracted and the vector is normalized to ensure that the constraint $E_b = \text{const}$ is satisfied. This vector represents the c_x component of the chaotic signals basis. The orthonormal component c_y is computed according to the FFT-based algorithm described in Sec. III-C.1. The basis signals c_x and c_y are then multiplied by $\sqrt{E_b}$ and used to form the reference and the information-bearing part of the QCSK signal. The latter is obtained by combining the chaotic basis vectors according to the constellations shown in Fig. 3.

A. Simulation Results

Fig. 4 shows a plot of the BER (bit error rate) versus E_b/N_0, where E_b represents the energy per bit and N_0 is the (unilateral) noise power spectral density. The performance curves refer to the signal constellations shown in Fig. 3, for $K = 2, 16, 64$.

The performance curves refer to the signal constellations shown in Fig. 3, for $K = 2, 16, 64$. Note that the DCSK1 and DCSK2 versions exhibits the same BER performance and the same can be said about QCSK1 and QCSK2. Then, we can conclude that the hypothesis made in Sec. IV-B on the noise component n' at the output of the Hilbert filter is verified. In particular, this confirms that the distribution of n' can be considered Gaussian and coinciding with n.

The simulations have been carried out using MATLAB and verified with the simulation package SYSTEMVIEW.

B. Dependence on the Correlation Time

As pointed out in [24], [25], [26], the performance of transmitted-reference communication schemes (such as DCSK and QCSK) depends on the correlation time K.[4] This property is confirmed by Fig. 4, which shows the

[4]With an abuse of notation we refer here to K as the correlation time, while it should be clear that K represents the length of the chaotic vectors c_x, c_y and m_s.

BER performance of the QCSK and DCSK schemes for different correlation times K. As visible from Fig. 4, the error probability increases as K is increased. Note also that for low values ($K < 16$) of the correlation time DCSK performs better than QCSK, while for higher values of K, QCSK outperforms DCSK. This result is explained in details in the next subsection.

C. Theoretical Analysis

The goal of this part of the work is to derive analytical expressions for the bit error rate of the QCSK scheme. In particular, we develop formulas expressing the BER in terms of probabilities of variables which are functions of standard Gaussian random variables. Then, by applying the central limit theorem [23] we find approximate analytical expressions of the BER valid for sufficiently large K. The key result for our analysis is expressed by Lemma 1 (in Sec. V-C.1), showing that the performance of the QCSK scheme does not depend on the particular choice of the reference signal. We will present the analysis for the discrete-time case, which can also be considered as a model of the continuous-time system, as previously mentioned.

C.1 BER Analytical Expressions

Let us assume that the reference signal consists of K chaotic samples, generated by a chaotic system with frequency f_s. The length of the information-bearing part is also K, resulting in a total of $2K$ samples per symbol and $T = 2Kt_s$, where $t_s = 1/f_s$. Correspondingly, by keeping into account that in QCSK two bits of information are associated to every symbol, the energy per bit E_b is given by:

$$E_b = \frac{t_s}{2}\left(\sum_{i=1}^{K} r_i^2 + \sum_{i=1}^{K} m_i^2\right) = \frac{t_s}{2}\left(||r||^2 + ||m||^2\right),$$

where $(r_1, \ldots, r_K)$ and $(m_1, \ldots, m_K)$ are the reference and information vectors, respectively. On the other hand, AWGN noise with spectral density N_0 translates into independent random Gaussian variables with variance σ^2 being added to each sample, where $\sigma^2 = N_0/(2t_s)$.

In this analysis we consider the constellation QCSK2 with the following symbol encoding:

Symbol	Bits	Reference	Message
0	$(0,0)$	a	$c(+a+b)$
1	$(0,1)$	a	$c(+a-b)$
2	$(1,0)$	a	$c(-a+b)$
3	$(1,1)$	a	$c(-a-b)$

where $c = 1/\sqrt{2}$. Since each sample is contaminated by AWGN, at the receiver we observe $a+\eta = (a_i+\eta_i)_{i=1}^K$ and $m+\xi = (m_i+\xi_i)_{i=1}^K$, where η_i and ξ_i are zero mean independent Gaussian random variables with variance σ^2. The first bit is detected by correlating $m+\xi$ with $a+\eta$. If the correlation result is larger than zero then the decision is taken that the transmitted bit was "0", otherwise "1". The second bit is detected by correlating $m+\xi$ with the Hilbert transform of $a+\eta$. Here we assume that the Hilbert transform of $a+\eta$ is $b+\eta'$, where η' is also a vector of independent random Gaussian variables with variance σ^2. The validity of this assumption has been discussed in Sec. IV-B.

Lemma 1: Let us assume that the QCSK reference signal and the orthogonal signal used for the transmission have always the same norm e (it follows that the energy per bit is kept constant). Then the bit error rate (or probability of error) is equal to:

$$\mathrm{BER}_{\mathrm{QCSK}} = P_{\mathrm{QCSK}}(E) = P\left(\frac{1}{\sqrt{2}}||a||^2 + \frac{1}{\sqrt{2}}\sigma(a+b)^T\eta + \sigma a^T\xi + \sigma^2\eta^T\xi < 0\right), \tag{14}$$

where a and b are arbitrary vectors such that $a^Tb = 0$, $||a|| = ||b|| = e$, while η and ξ are vectors of independent standard (i.e. zero mean and unity variance) Gaussian random variables.

Proof: In QCSK the error probability can be computed as

$$P_{\mathrm{QCSK}}(E) = \frac{1}{2}(P(E_1) + P(E_2)),$$

where $P(E_i)$ is the error probability for the ith bit. The latter can be computed as:

$$P(E_i) = \sum_{j=0}^{3} P(E_i|s=j)P(s=j),$$

where $P(E_i|s=j)$ is the conditional error probability in the ith bit under condition that the symbol j was transmitted, and $P(s=j)$ is the probability of emitting the symbol j.

From the operation of the receiver it follows that:

$$P(E_1|s=0) = P((a+\eta)^T(c(a+b)+\xi) < 0), \tag{15}$$
$$P(E_1|s=1) = P((a+\eta)^T(c(a-b)+\xi) < 0), \tag{16}$$
$$P(E_1|s=2) = P((a+\eta)^T(c(-a+b)+\xi) > 0), \tag{17}$$
$$P(E_1|s=3) = P((a+\eta)^T(c(-a-b)+\xi) > 0), \tag{18}$$
$$P(E_2|s=0) = P((b+\eta)^T(c(a+b)+\xi) < 0), \tag{19}$$
$$P(E_2|s=1) = P((b+\eta)^T(c(a-b)+\xi) > 0), \tag{20}$$
$$P(E_2|s=2) = P((b+\eta)^T(c(-a+b)+\xi) < 0), \tag{21}$$
$$P(E_2|s=3) = P((b+\eta)^T(c(-a-b)+\xi) > 0), \tag{22}$$

where $c = 1/\sqrt{2}$. First let us observe that the probabilities (17), (18), (20), (22) are equal to (16), (15), (21) and (19), respectively. This can be seen by multiplying the formulas inside the parentheses by -1 and observing that the random vector $-\xi$ has the same distribution as ξ.

From Lemma 3, which is proved in Appendix A, it follows that the distributions appearing in the equations (15), (16), (19) and (21) are all equal. Hence, the probabilities (15)–(22) are equal. They also do not depend on the particular choice of a and b, as long as a and b are orthogonal and have constant norm. Hence

$$\begin{aligned} P_{\mathrm{QCSK}}(E) &= P(E_1|s=0) = P((a+\eta)^T(c(a+b)+\xi) < 0) \\ &= P((a+\sigma\eta')^T(c(a+b)+\sigma\xi') < 0) \\ &= P(c||a||^2 + c\sigma(a+b)^T\eta' + \sigma a^T\xi' + \sigma^2\eta'^T\xi' < 0) \end{aligned}$$

where η' and ξ' are vectors of independent standard Gaussian variables. ■

Now let us express the error probability in terms of the energy per bit $E_b = 2t_s||a||^2/2 = t_s||a||^2$ and the noise spectral density $N_0 = 2t_s\sigma^2$. Since the BER performance does not depend on the particular choice of a and b, let us choose: $a = (||a||, 0, \ldots, 0)$ and $b = (0, ||a||, 0 \ldots, 0)$. The formula for the QCSK error probability reads then:

$$\mathrm{BER}_{\mathrm{QCSK}} = P_{\mathrm{QCSK}}(E) = P\left(\sqrt{\frac{E_b}{N_0}}(\eta_1 + \eta_2 + \sqrt{2}\xi_1) + \sum_{i=1}^{K}\eta_i\xi_i < -\sqrt{2}\frac{E_b}{N_0}\right) \tag{23}$$

where η_i, ξ_i are independent standard Gaussian variables.

Remark 1: Similarly for DCSK one can show that the error probability does not depend on the reference vector a and is equal to:

$$P_{\mathrm{DCSK}}(E) = P\left(||a||^2 + \sigma a^T(\eta+\xi) + \sigma^2\eta^T\xi < 0\right),$$

where again η_i, ξ_i are independent Gaussian variables with zero mean and unity variance. By taking into account that for the DCSK scheme $E_b = 2t_s||a||^2$ and choosing $a = (||a||, 0, \ldots, 0)$ we obtain:

$$\mathrm{BER}_{\mathrm{DCSK}} = P_{\mathrm{DCSK}}(E) = P\left(\sqrt{\frac{E_b}{N_0}}(\xi_1 + \eta_1) + \sum_{i=1}^{K}\eta_i\xi_i < -\frac{E_b}{N_0}\right). \tag{24}$$

where η_i, ξ_i are independent standard Gaussian random variables.

From the formulas (23) and (24) it is clear that the performance of both methods degrades with increasing K. In fact, for larger K the only modification is the larger number of terms of the form $\eta_i\xi_i$, which increase the error probability. These formulas can be used for computation of the BER curves for the QCSK and DCSK techniques. Since we know the analytical expressions for the densities of η_i and ξ_i we can evaluate the density of the variables $\sqrt{\frac{E_b}{N_0}}(\eta_1+\eta_2+\sqrt{2}\xi_1)+\sum_{i=1}^{K}\eta_i\xi_i$ and $\sqrt{\frac{E_b}{N_0}}(\xi_1+\eta_1)+\sum_{i=1}^{K}\eta_i\xi_i$ in terms of definite integrals. For the computation of probabilities (23) and (24) one may use numerical integration methods. In this work these probabilities have been estimated numerically by considering an ensemble of vectors $\eta_1,\ldots,\eta_K$, $\xi_1,\ldots,\xi_K$, according to the normal distribution $N(0,1)$, and applying the definition of probability as relative frequency associated with an observed event [9]. This approach is very accurate for moderate values of E_b/N_0. Note that for DCSK there exists an exact expression for bit error rate [24], [25], which gives results coinciding with those obtained using the above procedure.

In Fig. 5 we present a comparison of the theoretical predictions with the simulation results for a QCSK system based on the Renyi map. One can clearly see the perfect agreement. Fig. 6 shows the theoretical predictions for the BER, comparing QCSK versus DCSK. For low values of E_b/N_0, QCSK exhibits better BER performance than DCSK. For higher E_b/N_0 and small K, DCSK has lower error probability. For $K=16$ the BER curves are close to each other, while for larger K QCSK performs better than DCSK in the whole range of E_b/N_0.

C.2 Approximation Using the Central Limit Theorem

The central limit theorem [23] states that if $\{y_i\}_{i=1}^{N}$ are statistically independent zero mean random variables with the same probability density function and variance σ^2, and $z=\frac{1}{\sqrt{N}}\sum_{i=1}^{N}y_i$, then the distribution of z approaches Gaussian distribution with zero mean and variance σ^2 as N goes to infinity. We now use this result to develop approximate analytical expressions for the BER in QCSK (and DCSK).

In order to apply the central limit theorem we assume that K is even and we choose vectors

$$a=\frac{||a||}{\sqrt{K}}(1,1,\ldots,1),\quad b=\frac{||a||}{\sqrt{K}}(1,-1,\ldots,1,-1).$$

From Lemma 1 it follows that

$$P_{\mathrm{QCSK}}(E)=P\left(\frac{1}{\sqrt{2}}||a||^2+\frac{1}{\sqrt{2}}\sigma\sum_{i=1,i-odd}^{K}2\eta_i+\sigma\sum_{i=1}^{K}\xi_i+\sigma^2\sum_{i=1}^{K}\eta_i\xi_i<0\right). \tag{25}$$

Dividing the expression within the parentheses by σ^2 and taking into account that $||a||/\sigma=\sqrt{2E_b/N_0}$ we obtain:

$$P_{\mathrm{QCSK}}(E)=P\left(\sum_{i=1,i-\mathrm{odd}}^{K}\left(\sqrt{\frac{2E_b}{KN_0}}(\sqrt{2}\eta_i+\xi_1+\xi_{i+1})+\eta_i\xi_i+\eta_{i+1}\xi_{i+1}\right)<-\frac{\sqrt{2}E_b}{N_0})\right)$$

Let us define for $i=1,\ldots,K/2$

$$y_i=\sqrt{\frac{2E_b}{KN_0}}(\sqrt{2}\eta_{2i-1}+\xi_{2i-1}+\xi_{2i})+\eta_{2i-1}\xi_{2i-1}+\eta_{2i}\xi_{2i},$$

and

$$z=\sqrt{\frac{2}{K}}\sum_{i=1}^{K/2}y_i.$$

y_i are zero mean random variables with the same distribution and variance: $\sigma_y^2 = 2 + 8E_b/(KN_0)$. It follows that:

$$P_{\mathrm{QCSK}}(E) = P\left(\sqrt{\frac{K}{2}}z < -\frac{\sqrt{2}E_b}{N_0}\right) = P\left(z < -\frac{2E_b}{KN_0}\right).$$

For large K, the random variable z has approximately Gaussian distribution with variance σ_y, thus the probability of error can be computed as

$$P_{\mathrm{QCSK}}(E) = \frac{1}{2}\operatorname{erfc}\left(\frac{2E_b}{KN_0\sqrt{2}\sigma_y}\right) = \frac{1}{2}\operatorname{erfc}\left(\left(4\frac{N_0}{E_b} + K\frac{N_0^2}{E_b^2}\right)^{-1/2}\right), \tag{26}$$

where $\operatorname{erfc}(\cdot)$ is the complementary error function [23].

For DCSK this method gives the following expression:

$$P_{\mathrm{DCSK}}(E) = \frac{1}{2}\operatorname{erfc}\left(\left(4\frac{N_0}{E_b} + 2K\frac{N_0^2}{E_b^2}\right)^{-1/2}\right). \tag{27}$$

These approximations are valid for large correlation times K. Since the erfc is a strictly decreasing function it follows that for large K the QCSK method is better than DCSK in terms of error probability.

Fig. 6 shows the BER curves obtained by plotting formulas (26) and (27), for $K = 2, 16, 64$. As it can be seen in Fig. 6(c), the approximate results based on the central limit theorem and the exact curves tend to get closer for $K = 64$. For smaller values of K the error due to the assumption that the distribution of z is Gaussian causes unacceptable differences (see Fig. 6(b) and especially Fig. 6(a)). This fact is demonstrated by Fig. 7 showing that the distribution of $\sum_{i=1}^{k} y_i$, for small k, is far from Gaussian.

D. QCSK versus DCSK

Summarizing, QCSK may be considered equivalent to two DCSK systems: the first using the reference signal $c_x(t)$ and the second using the orthogonal signal $c_y(t)$ which is restored at the receiver from the reference part of the transmitted signal. The advantage of the proposed QCSK scheme is that there is no need to send the orthogonal signal over the channel as its estimate can be reproduced from the received reference signal. The price is the higher complexity as QCSK requires the generation of the complementary signal in both the transmitter and the receiver. The BER performances of the DCSK and QCSK schemes are similar but QCSK has double data rate. In fact the QCSK symbol consists of two bits as opposed to one bit in DCSK. Since the two signals occupy the same bandwidth it follows that QCSK has higher spectral efficiency with respect to DCSK.

VI. Extension to M-ary Constellations

In general QCSK may be extended to M-symbol constellations. For example, this can be obtained by considering the set of complex numbers: $m_s = e^{i2s\pi/M}$, $s = 1, \ldots, M$. This choice gives a chaos-based version of M-ary PSK (Phase Shift Keying). Moreover, if the constellation signals are not restricted to lie on a circle one can design a chaotic version of QAM (Quadrature Amplitude Modulation) [9]. In this case however the conditions $E_b = \text{const}$ is no longer satisfied.

VII. Conclusions

In this paper we have proposed a multilevel chaos-based modulation scheme called QCSK (Quadrature Chaos Shift Keying). The QCSK scheme is derived from DCSK and exhibits similar BER performance as DCSK but double data rate for a given bandwidth (or half bandwidth for given data rate), resulting in an increased spectral efficiency. The drawback consists in an increased complexity of both transmitter and receiver.

VIII. Acknowledgements

The authors would like to thank A. Abel, G Kolumbán and L. Tsimring for the stimulating discussions. This research was sponsored in part by the ARO, grant No. DAAG55-98-1-0269.

IX. Appendix A

In this Appendix we prove two lemmas, which are necessary for showing that the performance of the QCSK modulation method does not depend on the particular choice of the orthogonal signals a and b, as long as $||a|| = ||b|| = \text{const}$.

The following lemma shows that a linear transformation defined by an orthonormal matrix transforms a vector of independent Gaussian variables into a vector of random variables with the same properties.

Lemma 2: Let us assume that $\eta = (\eta_1, \dots, \eta_n)$ is a vector of independent Gaussian variables with zero mean and variance σ^2. Let T be an orthonormal matrix, i.e. $T^{-1} = T^T$ and rows of T have norm 1 ($\sum_{j=1}^n T_{ij}^2 = 1$ for $i = 1, \dots, n$). Let $\eta' = T\eta$. Then η' is a vector of independent Gaussian variables with zero mean and variance σ^2.

Proof: It is well known that a linear combination $z = a_1 x_1 + \cdots + a_n x_n$ of zero mean independent Gaussian random variables x_i, each with variance σ^2 is itself a zero mean Gaussian variable with variance $\sigma_z^2 = (a_1^2 + \cdots + a_n^2)\sigma^2$. It follows that $\eta_i' = \sum_{j=i}^n T_{ij}\eta_j$ is a zero mean random Gaussian variable with variance

$$\sigma_{\eta_i'}^2 = \sum_{j=i}^n T_{ij}^2 \sigma^2 = \sigma^2.$$

From the assumptions it follows that the joint probability density function of $\eta_1 \dots, \eta_L$ is equal to

$$p_{\eta_1 \dots, \eta_L}(\alpha_1, \dots, \alpha_L) = \prod_{i=1}^n \frac{1}{\sqrt{2\pi}\sigma} \exp\left(-\frac{\alpha_i^2}{2\sigma^2}\right).$$

We will show independence of η_i' using the theorem on reversible transformations of random vectors [27]. According to this theorem the joint density function of $\eta' = f(\eta)$ (where f is reversible, $g = f^{-1}$) can be computed as

$$p_{\eta_1' \dots, \eta_L'}(\beta) = |Dg(\beta)| p_{\eta_1 \dots, \eta_L}(g_1(\beta), \dots, g_n(\beta)),$$

where $\beta = (\beta_1, \dots, \beta_n)$.

In our case $\eta' = f(\eta) = T\eta$, $\eta = g(\eta') = T^T\eta$, the Jacobian of g is constant and its determinant is $|Dg(\beta)| = |T^T| = 1$.

$$\begin{aligned} p_{\eta'}(\beta) &= \prod_{i=1}^n \frac{1}{\sqrt{2\pi}\sigma} \exp\left(-\frac{g_i^2(\beta)}{2\sigma^2}\right) = \frac{1}{(\sqrt{2\pi}\sigma)^n} \exp\left(-\frac{\sum_{i=1}^n g_i^2(\beta)}{2\sigma^2}\right) = \frac{1}{(\sqrt{2\pi}\sigma)^n} \exp\left(-\frac{||T^T\beta||^2}{2\sigma^2}\right) \\ &= \frac{1}{(\sqrt{2\pi}\sigma)^n} \exp\left(-\frac{||\beta||^2}{2\sigma^2}\right) = \prod_{i=1}^n \frac{1}{\sqrt{2\pi}\sigma} \exp\left(-\frac{\beta_i^2}{2\sigma^2}\right) = \prod_{i=1}^n p_{\eta_i'}(\beta_i). \end{aligned}$$

Since the joint density function of $\eta' = (\eta_1', \eta_2', \dots, \eta_n')$ can be factorized in the form shown above it follows that the random variables η_i' are independent. ■

The next lemma states that the distributions of random variables appearing in the formulas (15)–(22) do not depend on a and b, as long as a and b are orthogonal and their Euclidean norms are equal and fixed.

Lemma 3: Let $\eta = (\eta_1, \dots, \eta_n)$ and $\xi = (\xi_1, \dots, \xi_n)$ be vectors of independent Gaussian variables with zero mean and variance σ^2. Let $n \geq 2$, $a = (a_1, \dots, a_n)$ and $b = (b_1, \dots, b_n)$. Let us assume that $||a|| = ||b||$ is constant and $a^T b = 0$. Then the random variable defined as

$$z = (a + \eta)^T ((a + b)/\sqrt{2} + \xi) \tag{28}$$

has a distribution which does not depend on a and b.

Proof: Let $c = 1/\sqrt{2}$. The distribution under consideration can be written as follows:

$$z = c||a||^2 + c(a+b)^T\eta + a^T\xi + \eta^T\xi$$

We skip the constant term $c||a||^2$. We show that the following distributions are the same

$$z = c(a+b)^T\eta + a^T\xi + \eta^T\xi, \tag{29}$$

$$\bar{z} = c||a||(\eta_1+\eta_2) + ||a||\xi_i + \eta^T\xi. \tag{30}$$

The first distribution is obtained using arbitrary vectors a and b, while the second is obtained for $a = (||a||, 0, \dots, 0)$, $b = (0, ||a||, 0, \dots, 0)$. First we split the random vector ξ into the sum of two independent random vectors, with components being random independent Gaussian variables with the same variance as ξ.

$$\xi = \frac{1}{\sqrt{2}}(\tilde{\xi} + \bar{\xi}) = c(\tilde{\xi} + \bar{\xi}).$$

After this substitution z can be rewritten as

$$z = c(a^T\eta + b^T\eta) + ca^T(\tilde{\xi} + \bar{\xi}) + c\eta^T(\tilde{\xi} + \bar{\xi}) = c(a^T\eta + b^T\eta + a^T\tilde{\xi} + a^T\bar{\xi} + \eta^T\tilde{\xi} + \eta^T\bar{\xi}). \tag{31}$$

Let $e_1 = \frac{a}{||a||}$ and $e_2 = \frac{b}{||b||}$. Let us choose vectors $e_3, \dots, e_n$ in such a way that $e_1, \dots, e_n$ is an orthonormal base in $\mathbb{R}^n$. Also, we define the square matrix $T = (e_1, e_2, \dots e_n)^T$. We now define $\eta' = T\eta$, $\tilde{\xi}' = T\tilde{\xi}$, $\bar{\xi}' = T\bar{\xi}$. Since T is an orthonormal matrix it follows from Lemma 2 that η', $\tilde{\xi}'$, $\bar{\xi}'$ are vectors of independent random variables with same distribution as η, $\tilde{\xi}$, $\bar{\xi}$.

We have the following relations:

$$\begin{aligned}
&\eta = T^T\eta', \quad \tilde{\xi} = T^T\tilde{\xi}', \quad \bar{\xi} = T^T\bar{\xi}',\\
&a^T\eta = a^TT^T\eta' = a^Te_1\eta'_1 = ||a||\eta'_1,\\
&b^T\eta = ||a||\eta'_2, \quad a^T\tilde{\xi} = ||a||\tilde{\xi}'_1, \quad a^T\bar{\xi} = ||a||\bar{\xi}'_1,\\
&\eta^T\tilde{\xi} = (T^T\eta')^TT^T\tilde{\xi}' = \eta'^TTT^T\tilde{\xi}' = \eta'^T\tilde{\xi}',\\
&\eta^T\bar{\xi} = \eta'^T\bar{\xi}'.
\end{aligned}$$

from which we obtain finally

$$z = c(||a||\eta'_1 + ||a||\eta'_2 + ||a||\tilde{\xi}' + ||a||\bar{\xi}' + \eta'^T\tilde{\xi}' + \eta'^T\bar{\xi}') = c||a||(\eta'_1+\eta'_2) + ||a||\xi'_1 + \eta'^T\xi',$$

where $\xi' = c(\tilde{\xi}' + \bar{\xi}')$ is a vector of independent random Gaussian variables with variance σ^2. Thus we have shown that the distributions (29) and (30) are the same. ■

References

[1] H. Dedieu and M.P. Kennedy amd M. Hasler, "Chaos shift keying: Modulation and demodulation of a chaotic carrier using self-synchronizing Chua's circuits," *IEEE Trans. Circ. Syst. II*, vol. 40, no. 10, pp. 634–642, 1993.

[2] S. Hayes and C. Grebogi, "Using chaos for digital communication," in *Nonlinear Dynamics in Circuits*, T. Carroll and L. Pecora, Eds., pp. 325–335. World Scientific, 1995.

[3] G. Kolumbán, M.P. Kennedy, and L.O. Chua, "The role of synchronization in digital communication using chaos — Part I: Fundamentals of digital communication," *IEEE Trans. Circ. Syst. I*, vol. 44, no. 10, pp. 927–935, 1997.

[4] G. Kolumbán, M.P. Kennedy, and L.O. Chua, "The role of synchronization in digital communication using chaos — Part II: Chaotic modulation and chaotic synchronization," *IEEE Trans. Circ. Syst. I*, vol. 45, no. 11, pp. 1129–1140, 1998.

[5] G. Kolumbán, G. Kis, Z. Jákó, and M.P. Kennnedy, "FM-DCSK: A robust modulation scheme for chaotic communications," *IEICE Trans. on Fundamentals of Electronics, Communications and Computer Sciences*, vol. E-81A, pp. 1798–1802, 1998.

[6] M. Sushchik, N. Rulkov, L. Larson, L. Tsimring, H. Abarbanel, K.Yao, and A. Volkovskii, "Chaotic pulse modulation: a robust method of communication with chaos," *IEEE Communication Letters*, vol. 4, pp. 128–130, 2000.

[7] Z. Galias and G.M. Maggio, "Quadrature chaos shift keying," in *Proc. IEEE Int. Symposium on Circuits and Systems, ISCAS'01*, Sydney, May 2001.

[8] G. Kolumbán and G. Kis, "Multipath performance of FM-DCSK chaotic communications system," in *Proc. IEEE Int. Symposium on Circ. and Syst., ISCAS'00*, Geneva, 2000, pp. 433–436.

[9] L.W. Couch, *Digital and analog communication systems*, Prentice Hall, New Jersey, 1997.

[10] G. Kolumbán and M.P. Kennedy, "The role of synchronization in digital communication using chaos—Part III: Performance bounds for correlation receivers," *IEEE Trans. Circ. Syst. I*, vol. 47, no. 12, pp. 1673–1683, 2000.

[11] G. Kolumbán, P. Kennedy, and G. Kis, "Multilevel differential chaos shift keying," in *Proc. Int. Workshop, Nonlinear Dynamics of Electronics Systems, NDES'97*, Moscow, 1997, pp. 191–196.

[12] M.P. Kennedy, G. Kolumbán, G. Kis, and A. Jákó, "Recent advances in communication with chaos," in *Proc. IEEE Int. Symposium on Circ. and Syst., ISCAS'98*, Monterey, 1998, pp. 461–464.

[13] E.A. Lee and D.G. Messerschmitt, *Digital communications*, Kluwer Academic, Boston (MA), 2nd edition, 1993.

[14] J.H. McClellan, T.W. Parks, and L.R. Rabiner, "A computer program for designing optimum FIR linear phase digital filters," *IEEE Trans. Audio Electroacoust.*, vol. AE-21, pp. 506–526, Dec. 1973.

[15] S.C. Pei and J.J. Shyu, "Design of FIR Hilbert transformers and differentiators by eigenfilter," *IEEE Trans. Circ. Syst.*, vol. 35, pp. 1457–1461, Nov. 1988.

[16] S. Sunder and V. Ramachandran, "Design of equiripple nonrecursive digital differentiators and Hilbert transformers using weighted leastsquares technique," *IEEE Trans. Signal Processing*, pp. 2504–2509, Sept. 1994.

[17] K.P. Pun, J.E. Franca, and C.A. Leme, "Polyphase SC IIR Hilbert transformer," *Electron. Lett.*, vol. 35, pp. 689–690, Apr. 1999.

[18] A. Hiroi, K. Endo, H. Kamata, and Y. Ishida, "Design and implementation of an ideal Hilbert transformer using neural networks," in *Proc. IEEE Pacific Rim Conf. Communication, Computer and Signal Processing*, 1993, vol. I, pp. 292–295.

[19] S. Samadi, Y. Igarashi, and H. Iwakura, "Design and multiplierless realization of maximally flat FIR digital Hilbert transformers," *IEEE Trans. Signal Processing*, vol. 47, pp. 1946–1953, July 1999.

[20] M. Simon and G.R. Tomlinson, "Use of the Hilbert transform in modal analysis of linear and non-linear structures," *Journal of Sound and Vibration*, vol. 96, no. 4, pp. 421–436, 1984.

[21] A. Reilly, G. Frazer, and B. Boashash, "Analytical signal generation—Tips and traps," *IEEE Trans. Signal Processing*, vol. 42, no. 11, pp. 3241–3245, 1994.

[22] S.D. Bedrosian, "Normalized design of 90 degree phase difference networks," *IRE Trans. Circuit Theory*, pp. 128–136, 1960.

[23] J.G. Proakis, *Digital communications*, McGraw-Hill, New York, 3rd edition, 1995.

[24] G. Kolumbán, "Theoretical noise performance of correlator-based chaotic communication schemes," *IEEE Trans. Circ. Syst. I*, vol. 47, no. 12, pp. 1692–1701, 2000.

[25] A. Abel, W. Schwarz, and M. Götz, "Noise performance of chaotic communication systems," *IEEE Trans. Circ. Syst. I*, vol. 47, no. 12, pp. 1726–1732, 2000.

[26] M. Sushchick, L.S. Tsimring, and A.R. Volkovskii, "Performance analysis of correlation-based communication schemes utilizing chaos," *IEEE Trans. Circ. Syst. I*, vol. 47, no. 12, pp. 1684–1691, 2000.

[27] J.M. Wozencraft and I.M. Jacobs, *Principles of communication engineering*, John Wiley & Sons, New York, 1990.

List of Figures

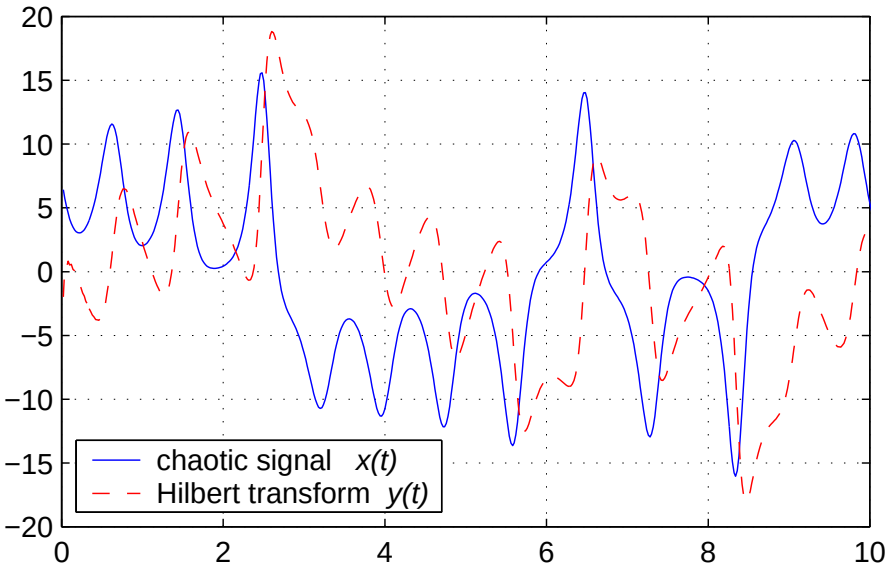

Fig. 1. Example of chaotic waveform $x(t)$ and corresponding orthogonal signal $y(t)$, computed by taking the Hilbert transform of $x(t)$ over the interval $[0, 10]$.

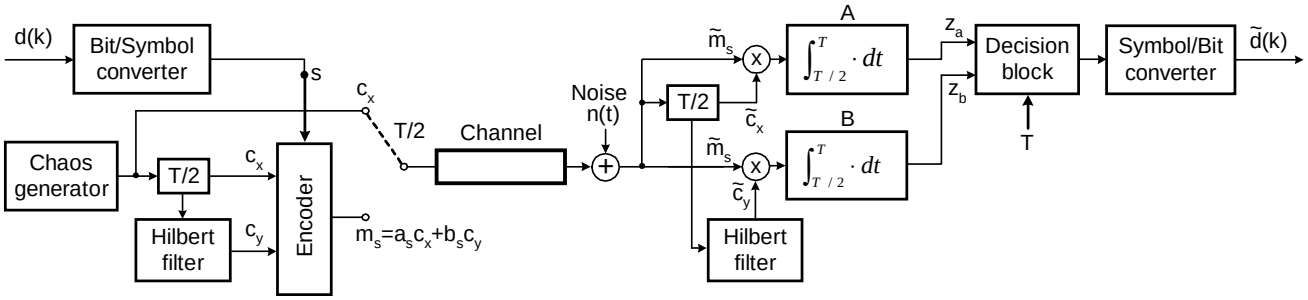

Fig. 2. Simplified block diagram of the QCSK scheme. Please refer to the text for a detailed description of its operation.

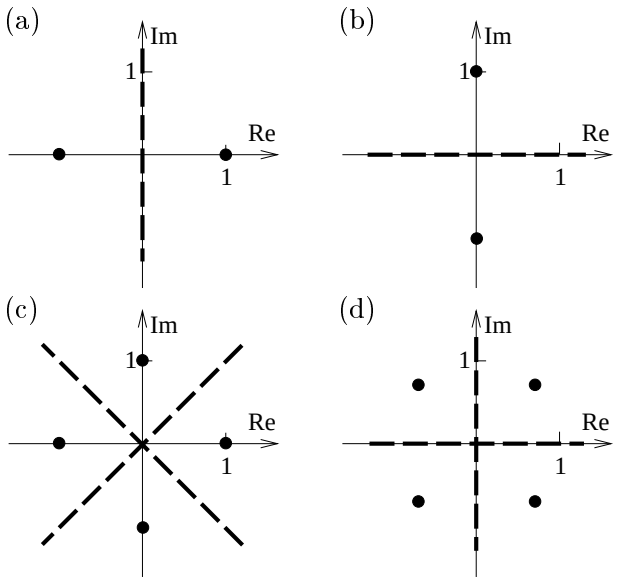

Fig. 3. Chaotic constellations. Two-level signaling: (a) DCSK1 and (b) DSCK2. Four-level signaling: (c) QCSK1 and (d) QCSK2. The dashed lines represent the decision boundaries.

(a)

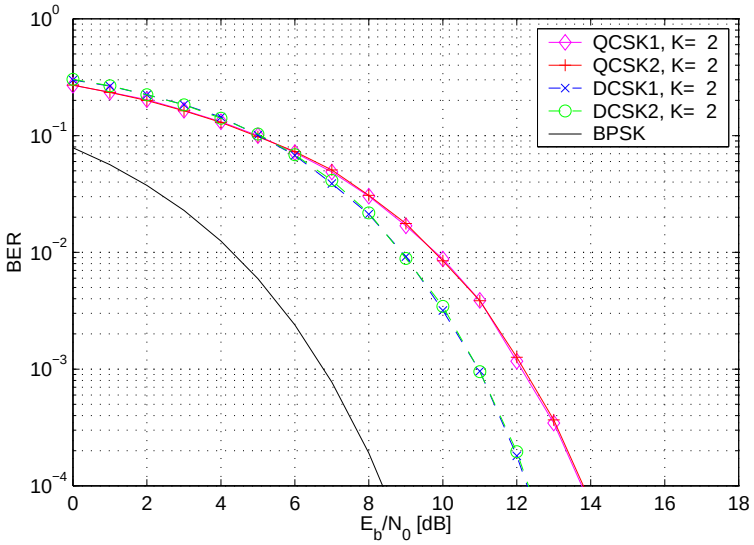

(b)

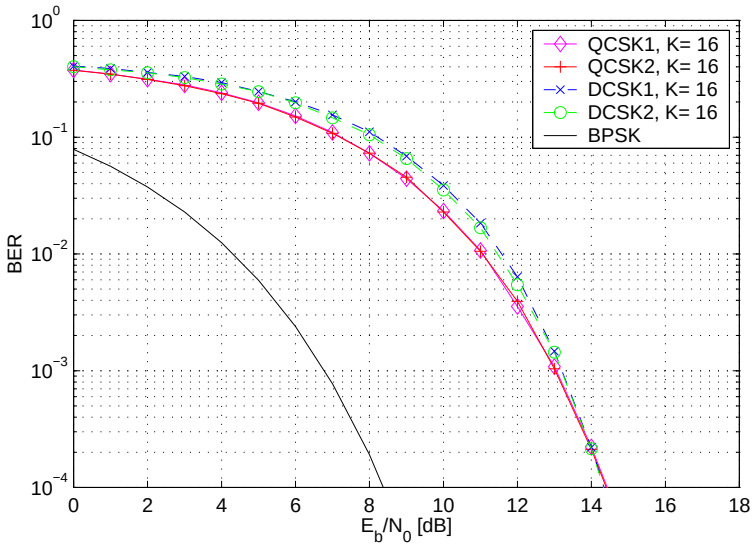

(c)

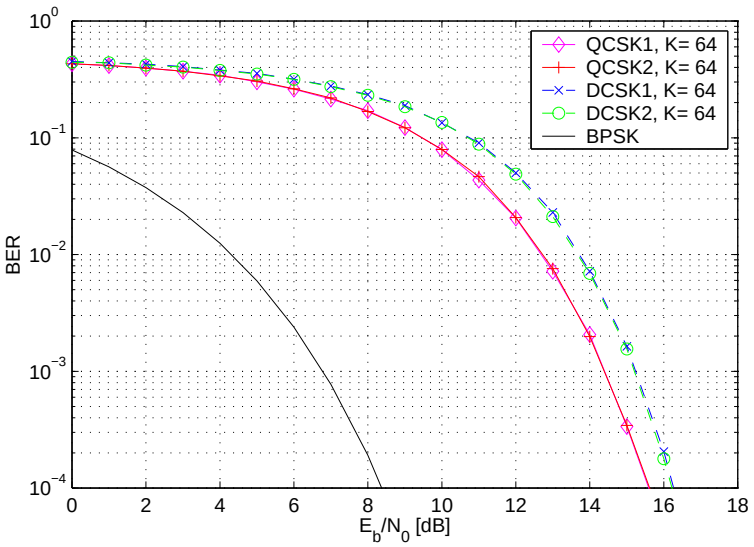

Fig. 4. Comparison of BER performance: QCSK versus DCSK. (a) $K = 2$, (b) $K = 16$, (c) $K = 64$. The results for QCSK and DCSK are plotted with solid and dashed lines, respectively. Note that for sufficiently large values of K (> 16) QCSK outperforms DCSK.

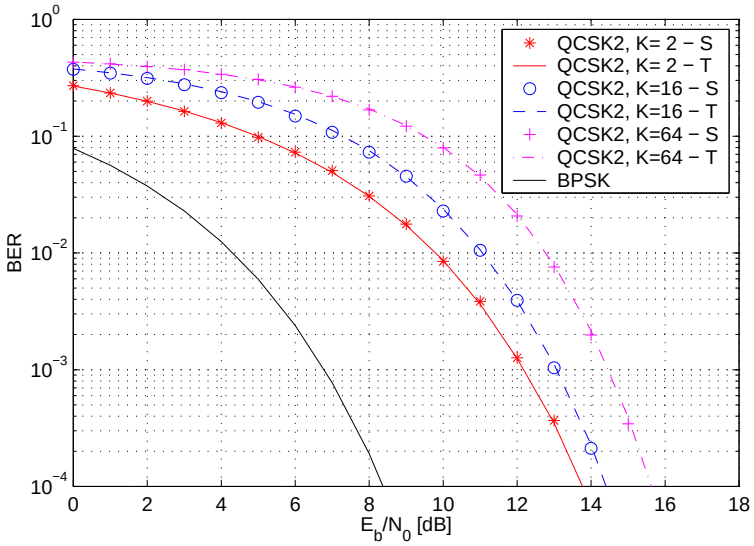

Fig. 5. Bit error rate for the QCSK modulation (version QCSK2). Comparison of simulation results (S) and theoretical predictions (T) for $K = 2, 16, 64$.

(a)

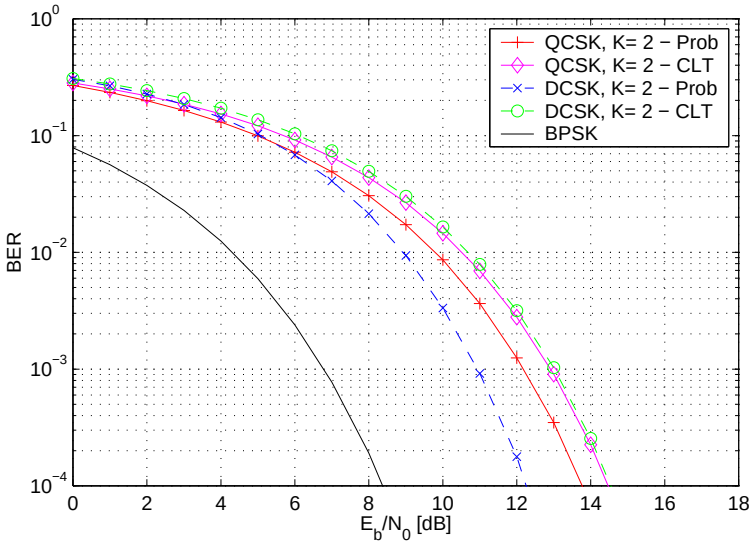

(b)

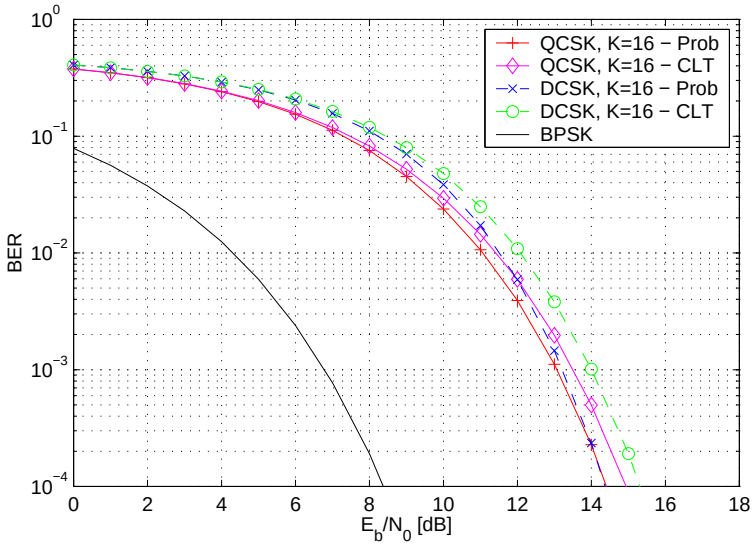

(c)

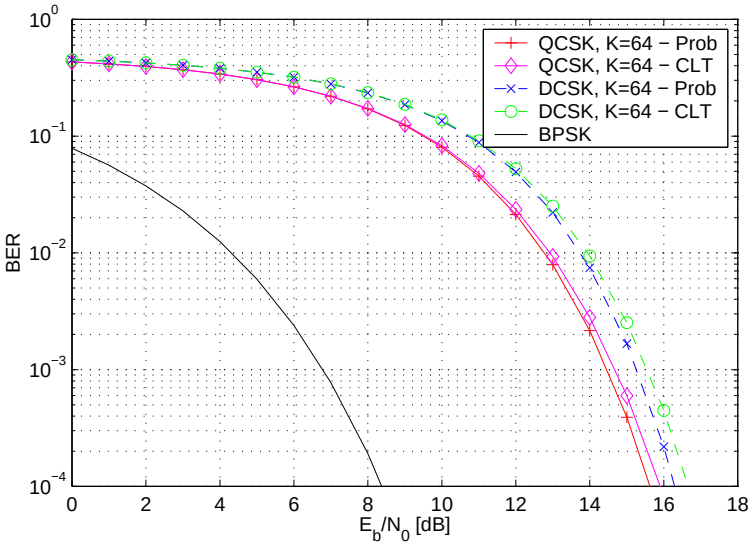

Fig. 6. BER plots for QCSK and DCSK obtained using the exact formulas (23) and (24) and the approximate formulas derived using the central limit theorem for: (a) $K = 2$, (b) $K = 16$, (c) $K = 64$. For small K the DCSK scheme shows better performance, for $K = 16$ the performance is approximately the same, while for larger K the QCSK scheme has smaller error probability in the whole range of E_b/N_0.

(a)

(b)

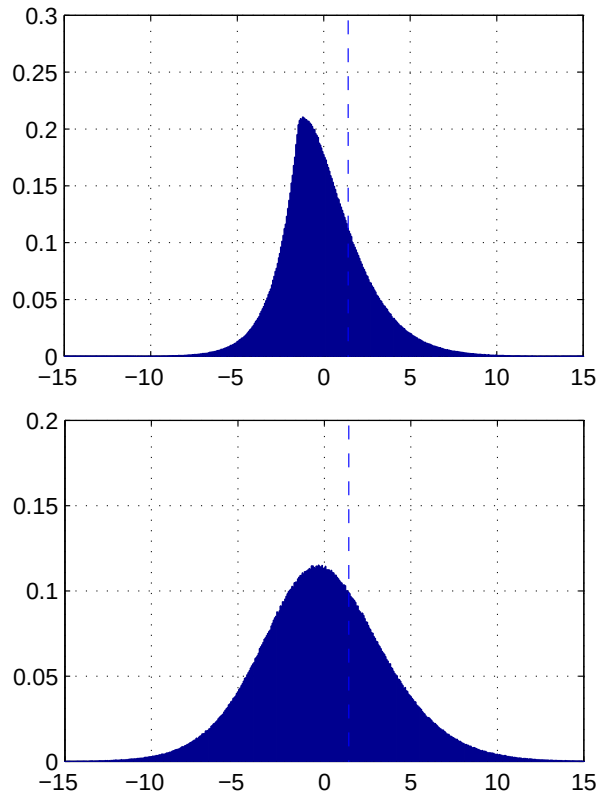

Fig. 7. Probability density function of $\sum_{i=1}^{k} y_i$, where $y_i = \sqrt{2}\eta_{2i-1} + \xi_1 + \xi_2 + \eta_{2i-1}\xi_{2i-1} + \eta_{2i}\xi_{2i}$ with ξ_i and η_i being random variables with normal distribution $N(0,1)$, for: (a) $k = 1$ and (b) $k = 5$.